6-1-2023

# Simulated temperatures of forest fires affect water solubility in soil and litter

Konrad Miotliński
*Edith Cowan University*

Kuenzang Tshering
*Edith Cowan University*

Mary C. Boyce
*Edith Cowan University*

David Blake
*Edith Cowan University*

Pierre Horwitz
*Edith Cowan University*



10.1016/j.ecolind.2023.110236
Miotliński, K., Tshering, K., Boyce, M. C., Blake, D., & Horwitz, P. (2023). Simulated temperatures of forest fires affect water solubility in soil and litter. *Ecological Indicators*, 150, Articles 110236.
https://doi.org/10.1016/j.ecolind.2023.110236

Ecological Indicators 150 (2023) 110236

Contents lists available at ScienceDirect

Ecological Indicators

journal homepage: www.elsevier.com/locate/ecolind

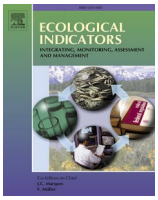

Original Articles

# Simulated temperatures of forest fires affect water solubility in soil and litter

Konrad Miotliński *, Kuenzang Tshering, Mary C. Boyce, David Blake, Pierre Horwitz

*Edith Cowan University, School of Science Centre for People, Place and Planet, 270 Joondalup Drive, Joondalup, WA, Australia*

ARTICLE INFO

*Keywords:*
Wildfire
Biogeochemical cycle
Metal contamination
Nutrient contamination
Carbonate formation

ABSTRACT

As wildfires are of increasing concern in a warming world, there is a need to understand how fire temperatures affect solute concentrations of forest litter and soils in drinking water catchments. In addition, the concentrations are expected to be affected by time since the previous fire. We sampled soil and litter from recently (2 months) and less recently (4.5 years) burnt sites from jarrah forest in SW Australia. The samples were heated at 250°C, 350°C, and 500°C for 30min followed by leaching to determine solute compositions at these temperatures and in unburnt samples. At 250°C–350°C, we found increased concentrations of manganese (Mn), arsenic (As), total phosphorus (TP), phosphate ($PO_4^{3-}$), ammonia ($NH_4^+$), potassium (K), calcium (Ca), mangesium (Mg), cobalt (Co), barium (Ba), sulphate ($SO_4^{2-}$), alkalinity and dissolved organic carbon in soils, as well as of zinc (Zn), As, Ca, Ba, alkalinity, aluminium (Al) and chromium (Cr) in litter. At 350°C–500°C, divalent cations and organic carbon declined, while soils generated very high Al and Cr concentrations. The time following the fire was important, with the more recent fire generating higher concentrations. The elevated concentrations in 250°C–350°C were attributed to a decomposition of organic matter and mineral transformations, including $CaCO_3$ formation. Based on thermodynamics, we propose a couple of burn severity indicators: activities of calcium and carbonates that are calculated from pH, alkalinity and Ca concentration. The indicators do not only show the degree of post-fire transformations, but they also inform on $CaCO_3$ formation. Further studies include: (1) application to field data, (2) association with organic contaminants, and (3) validation in other geographical locations.

## 1. Introduction

A continuing and rapid trend of hotter and more frequent wildfires poses a risk of polluting drinking water supplies (Abram et al., 2021; Robinne et al., 2021; Raoelison et al., 2023). One of the strategies to prevent the occurrence of deadly and destructive wildfires is to perform regular, low-temperature burns to reduce biomass load, maintain soil stability, and retain sensitive ecosystem components (Archibald et al., 2018; McLauchlan et al., 2020).

Since relatively mild temperature variations affect biogeochemical cycle rates of major elements in water (Mooshammer et al., 2017; Pellegrini et al., 2018), there is a need to understand how the elemental stocks are affected by burns of varying temperatures in forested catchments. The stocks may be either reduced with gas emissions (Newland et al., 2022) or augmented through deposition of post-fire debris (Bodí et al., 2014; Roshan and Biswas, 2023). Even in soils not affected by fire, the temperature shifts as little as 15°C completely reshuffle phase transformation, protein depolymerisation as well as biomass and inorganic stocks (Mooshammer et al., 2017). The post-fire processes tend to affect major and micro element cycling and they reveal (1) enhanced rates of organic matter decomposition (Pellegrini et al., 2022), (2) mineral dissolution (Johnston et al., 2019), (3) solid phase alterations (Burton et al., 2019; Johnson et al., 2015), and (4) precipitation of minerals including carbonates (Bodí et al., 2014; Nagra et al., 2017; Úbeda et al., 2009). The residual water and subsequent rainfall determine directions and magnitude of the effects on water quality of these processes (Li et al., 2020; Robinne et al., 2021).

The burnt vegetation is normally considered as a main source of dissolved contamination following a wildland fire (Campos et al., 2016; Nunes et al., 2018), while the chemical composition of ashes is vegetation specific (Yusiharni and Gilkes, 2012; Bodí et al., 2014). Soils, however, significantly change their physical and biogeochemical

* Corresponding author.
*E-mail address:* k.miotlinski@ecu.edu.au (K. Miotliński).

https://doi.org/10.1016/j.ecolind.2023.110236
Received 13 January 2023; Received in revised form 5 April 2023; Accepted 7 April 2023
Available online 23 April 2023

properties under elevated temperatures (Mooshammer et al., 2017; Alcaniz et al., 2018; Pellegrini et al., 2022; Roshan and Biswas, 2023). Firstly, upon heating soil infiltration is affected due to hydrophobic (water repellency) effects and due to hyper-dry conditions (Moody and Ebel, 2012). Furthermore, changes in infiltration patterns may result in preferential flow mechanism and erosion (Mao et al., 2019). Secondly, soil may become a contamination source, with, and even without, visible erosion (Robinne et al., 2021; Roshan and Biswas, 2023). A targeted extraction showed that the high severity wildfire at Wundowie, SW Australia, significantly changed the mineralogical composition of the lateritic soils by (1) dehydrating kaolinite, (2) converting gibbsite into boehmite and amorphous alumina, as well as (3) transforming goethite into maghemite/hematite (Yusiharni and Gilkes, 2012). These soils became depleted in total N and C, but enriched in phosphorus and potassium (Yusiharni and Gilkes, 2012). Johnston et al. (2019) in laboratory experiments showed that at the temperatures >400°C most of least stable iron oxides (ferrihydrite and goethite) present in soils get transformed to the more stable phases (hematite and maghemite) which triggered As mobilisation. A similar trigger was responsible for $Cr^{6+}$ mobilisation at 250°C–350°C in a laboratory study (Burton et al., 2019).

Time since the previous fire is likely to have different affects on water quality. Firstly, high nutrient availability after fire may explain higher leaf area index (LAI) increases (Boer et al., 2008). However, if fire frequency increases, the fuel load (Archibald et al., 2018), soil stability (McLauchlan et al., 2020), and biogeochemical functioning of forests (Pellegrini et al., 2018; Mishra et al., 2021) are affected. In a year without fire, as aboveground biomass dies and leaf litter decomposes, the forest releases stocks back into the soils. But in a year with a fire, the litter and plant biomass are combusted, leaving little plant mass to decompose into the soil. Over multiple years and repeated burning, carbon and nitrogen stocks decline by 36% and 38%, respectively, although other elements may remain unaffected (Pellegrini et al., 2018). Muqaddas et al. (2015) found that a wet sclerophyll forest burnt every 2 years is significantly depleted of C and N stocks when compared with the forest burnt every 4 years.

Ecological indicators for wildfire environs are urgently needed. Widely used indicators include pH (Bodí et al., 2014; Fajković et al., 2022; Raoelison et al., 2023), salinity (Roshan and Biswas, 2023), dissolved organic carbon (DOC, Santos et al., 2019; Chen et al., 2022; Tshering et al., 2023) and polycyclic aromatic hydrocarbons (PAHs, Santos et al., 2019; Chen et al., 2022; Tshering et al., 2023). Although very useful, none of these indicators can be used alone to determine the degree of fire severity and, consequently, overall water quality shifts and consequences. There are at least a couple of reasons for this. Firstly, there are no consistent sampling protocols for challenging post-wildfire environs resulting in contradictory results (Roshan and Biswas, 2023; Raoelison et al., 2023). This problem supports a need for more targeted experiments. Secondly, there are site specific processes that may affect indicators. For example, although pH normally increases after fires due to the dissolution of ashes, it may also decline due to carboxyl groups present in burned residues and wet deposition of dissolved acids (Raoelison et al., 2023). This means that pH may need to be analysed with other parameters in order to understand the degree of post-fire transformations. Moreover, good indicators should be efficient across scales (Stegen, 2018) and independent on burnt material (Nunes et al., 2018; Abram et al., 2021; Robinne et al., 2021).

To derive indicators thermodynamic theories can be used (Demirel and Gerbaud, 2019). They have been widely applied in geochemistry (Postma, 1983; Mongin et al., 2016; Li et al., 2021), biotechnology (Lee et al., 2019) and material engineering (Clavijo et al., 2022). The local thermodynamic equilibrium uses solute composition, ionic strength, and pH in determining the governing processes and ionic associations. For example, Postma (1983) by evaluating $Ca^{2+}$ and $SO_4^{2-}$ concentrations along a vertical soil profile identified a depth of gypsum accumulation. Similarly, calculations of solute saturation in highly concentrated leachate are used to predict mineral stability in waste disposal sites that undergo bio-remediation (Manning and Hillel, 2005).

We pursue a hypothesis-driven investigation that low temperature fires generate elevated solute concentrations. This is investigated through laboratory heating of soil and litter from a frequently burnt, low nutrient Australian forest. Then, we illustrate how thermodynamic indicators (1) inform on burn severity and (2) point to possible mineral associations. We further hypothesise that post-burn soils may be a significant contamination source and that a shorter time since the last fire results in higher concentrations per mass burnt.

## 2. Materials and methods

### 2.1. Study site and sampling

The study site located in SW Australia, in northern jarrah forest, 25 km SE from Perth, forms a forested catchment used for drinking water supply (116°4'20"E, 32°2'50"S). The region is a part of the Korung National Park, which has not undergone any significant clearing of native forest vegetation.

The forest is dominated by jarrah trees *(Eucalyptus marginata)*, with admixtures of marri *(Corymbia calophylla)*, yarri *(Eucalyptus patens)*, and bullich *(Eucalyptus megacarpa)* (Dell and Havel, 1989; Havel, 1989). The major understorey tree species are *Banksia grandis* and *Allocasuarina fraseriana* (Havel, 1989).

The soils of northern jarrah forest reflect the geology of the Yilgarn Craton, one of the oldest geological formations in the world, which has been exposed to sub-aerial conditions since the Late Proterozoic (Anand et al., 2019; Anand and Gilkes, 1987). Consequently, the soil consists of highly weathered materials that became depleted of many nutrient elements (Churchward and Dimmock, 1989; Yusiharni and Gilkes, 2012; Eldridge et al., 2018). At the study site, the alluvium sediments are composed of yellow siliceous sands and loose, regular ferruginous gravels. Occasionally, fragments of eroded laterite duricrust are found. The organic layer is up to 3 cm thick.

The soil and litter samples were collected in November 2020 at the interface of two controlled burns: a very recent one (September 2020, referred as recent), and a less recent (April 2016, referred as older) one (Fig. 1). The litter duff layer in both cases was 3 cm thick, although it could be more compacted for the older burnt. The recent burn was shortly after a wet season when there may have occasional rain and infiltration.

The samples were taken from 3 random sites at a maximum 100m distance between the recent and older burns. The soil was sampled up to a 5 cm depth underneath the litter layer. At each site, 5 replicates were taken, each from an area of $1m^2$. Upon removal of foreign material (small insects and macropod scats), all samples were subsequently stored at 4°C.

### 2.2. Sample preparation and heating

The samples were dried at temperatures 60°C and 105°C for litter and soil, respectively, for at least 24h until no change in mass was detected (Coughlan et al., 2002). Then, the grains greater than 2mm in the soil samples were removed by sieving, while the litter samples were crushed for homogenising. Each sample was divided into four 15g subsamples: a single sample to be thermally untreated (U) and three samples to be treated at the temperatures 250°C, 350°C, and 500°C. The choice of the temperatures roughly corresponds with low-, medium-, and high- burn intensities, respectively (Bradstock and Auld, 1995).

To perform the treatment, the furnace was heated to a set temperature and then the samples were placed in the furnace for a duration of 30min. Then, the untreated and treated samples were placed into bottles with deionised water (500 ml) followed by a single manual shake and stored for 24h at the room temperature. Then, the liquid was sampled with a syringe for a chemical analysis.

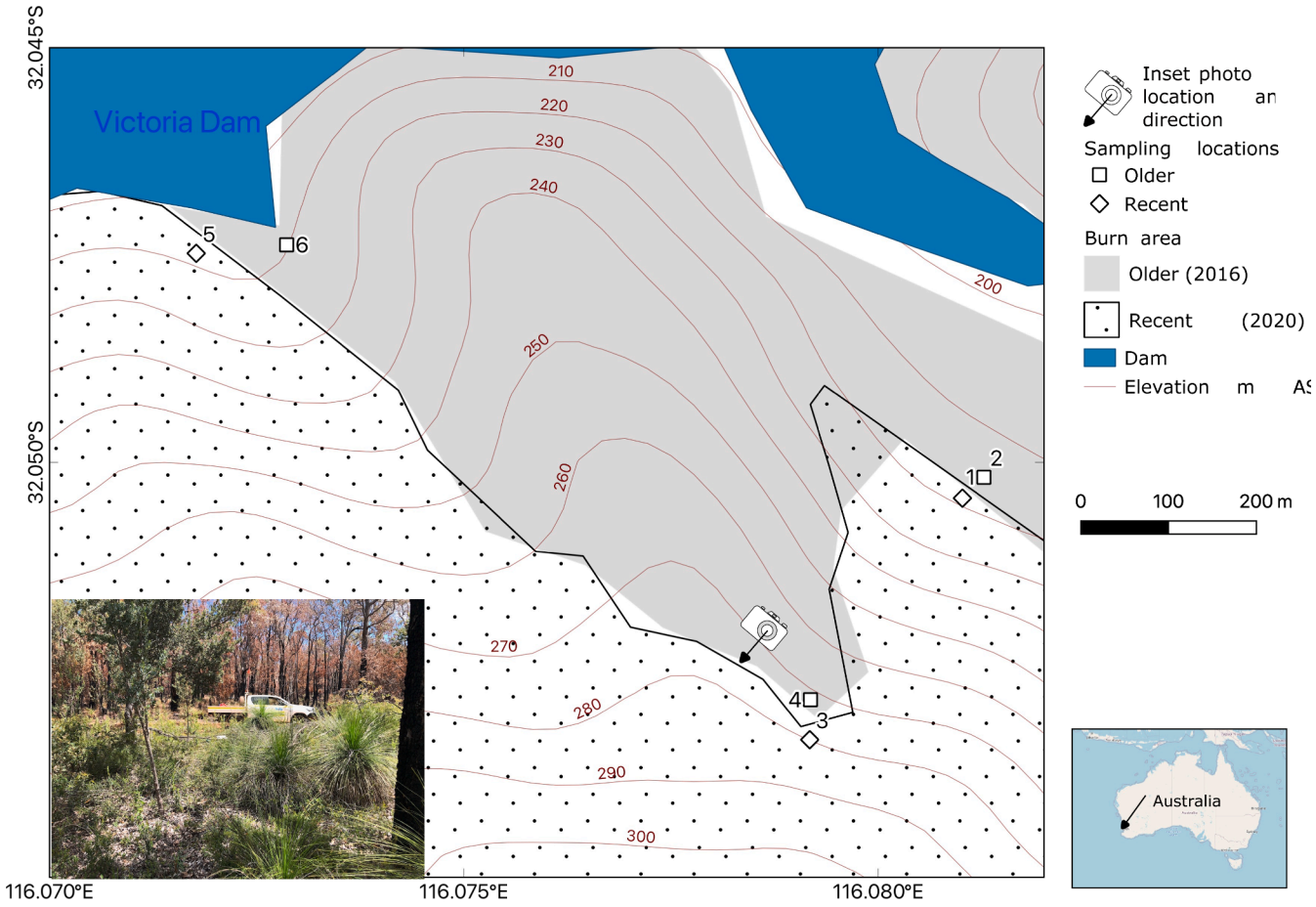


**Fig. 1.** The map of the sampling sites with odd numbers representing the recent burn and even numbers representing the older burn. The inset photograph shows the interface.

### 2.3. Chemical analyses

The liquid sample was divided into four subsamples for: (1) pH, (2) alkalinity (Alk), (3) total nitrogen (TN), and total phosphorus (TP), and (4) remaining solutes, including metals, dissolved organic carbon (DOC), and ultraviolet (UV) absorbance. The latter subsample was filtered through a 0.45μm cellulose acetate filters, while others remained unfiltered. Upon filtration the filtered subsamples were preserved with 2% (v/v) 7 M $HNO_3$ solution. pH was measured with a laboratory pH meter and alkalinity was determined by Gran titration with 0.2 N $H_2SO_4$ in an automatic titrator (Stumm and Morgan, 2013). The remaining leachate (extract) samples were stored in polyethylene bottles at 4°C for further analyses. Major and minor cations and total sulphur were measured by ICP-OES. Sulphate and chloride were measured by ion chromatography, DOC with the Shimadzu analyser, while TN and TP with the Lachat Flow Injection Nutrient analyser. The UV absorbance at wavelength of 254nm was determined using the Bench Top N6000 UV–vis Spectrophotometer.

### 2.4. Data and statistical processing

The parameters were subject to analysis through two way analysis of variance (Davis, 2002). The aim was to determine statistical significance of the temperatures, separately, once for litter and once for soil, the time since last fire, and the interactions between them on chemical parameters of extracts.

### 2.5. Mineralogical analysis

Selected soil and litter samples (4B and 5E for the older and recent burn, respectively) were subject to mineralogical analyses. Firstly, dry and crushed samples were treated with 3 M HCl to detect a presence of carbonate minerals. Secondly, X-ray diffraction was performed on the soil samples with the Empyrean range Malvern Panalytical instrument, which was subsequently interpreted with an open source Profex 5.0.0 software (Doebelin and Kleeberg, 2015).

### 2.6. Thermodynamic calculation

PHREEQC (Parkhurst and Appelo, 2013) was used to calculate: (1) ionic strength, and (2) ionic activities. Activity coefficients for solutes were calculated using the Debye-Hückel theory. Initially, the ionic strength ($I$) was calculated (Appelo and Postma, 2005; Stumm and Morgan, 2013):

$$I = \frac{1}{2}\sum(m_i/m_i^0 \cdot z_i^2) \equiv \frac{1}{2}\sum m_i \cdot z_i^2 \quad (1)$$

where $z_i$ is the charge number of ion $i$, and $m_i$ is the molality of $i$. The ionic strength becomes dimensionless by division with the standard state $m_i^0$ (1 mol $kg^{-1}$ $H_2O$).

Then, the ion activities for the i-th ion ($\gamma_i$) were calculated (Appelo and Postma, 2005; Stumm and Morgan, 2013):

$$log\gamma_i = -\frac{Az_i^2\sqrt{I}}{1 + Bå_i\sqrt{I}} \quad (2)$$

where $A$ and $B$ are temperature dependent constants; at 25°C $A$ =

0.5085, $B = 0.3285 \times 10^{10}$/m and $\dot{a}$ is a ion-size parameter. Eq. 2 is valid for dilute ($I < 0.1$) electrolyte solutions while alternative formulas exist for more concentrated solutions (Appelo and Postma, 2005).

The ion activities were then used as a proxy for mineral transformations (Demirel and Gerbaud, 2019). This is based on a principle that a solution in contact with a mineral phase tends to react with it depending on saturation (Appelo and Postma, 2005; Mongin et al., 2016). If a solution is undersaturated with respect to a phase, dissolution is feasible. If a solution is oversaturated, precipitation is feasible. The approach neither considers kinetics, the presence of precipitation inhibitors, nor a phase residuum following dissolution (Appelo and Postma, 2005; Santucci and Scully, 2020).

## 3. Results

The experiment was a two step procedure, heating and dissolution, that are caused by: *temperature* and *water*, respectively. Firstly, the temperature resulted in darkening of the treated matter without formation of the white ash. Total mass losses were 8% to 12% and 40% to 56% for soil and litter, respectively (Appendix A). Secondly, the $CO_2$-saturated water reacted through dissolution.

The effect of *Temperature* on water solubility is pronounced for both soil and litter exemplified in Fig. 2 with full treatment of parameters shown in Appendix B. The measured parameters can be distinguished into three categories:

1. highest concentration or value for *untreated* samples. The example includes Total Nitrogen (TN) and Mn in litter (Fig. 2), but also Fe, $NO_x$, Pb and UV absorbance in both soil and litter (Appendix B).
2. highest concentration or value at the *intermediate temperatures*. The example includes TN, Mn and $PO_4^{3-}$ in soil, Al in litter, and Ca both in soil and litter (Fig. 2). A similar pattern was identified for most cations that are soluble in water in the divalent form (2+), UV absorbance, and Alkalinity, $NH_4^+$, and $SO_4^{2-}$ in soils (Appendix B).
3. highest concentration or value at the *highest temperature*. The example includes Al in soil (Fig. 2) and and pH, Cr in soils, and $SO_4^{2-}$ in litter (Appendix B).

For the category 2, exhibiting concentration peaks in the studied temperature range, there are at least two different groups of mechanisms controlling concentrations: (1) net solute accumulation, when the con-

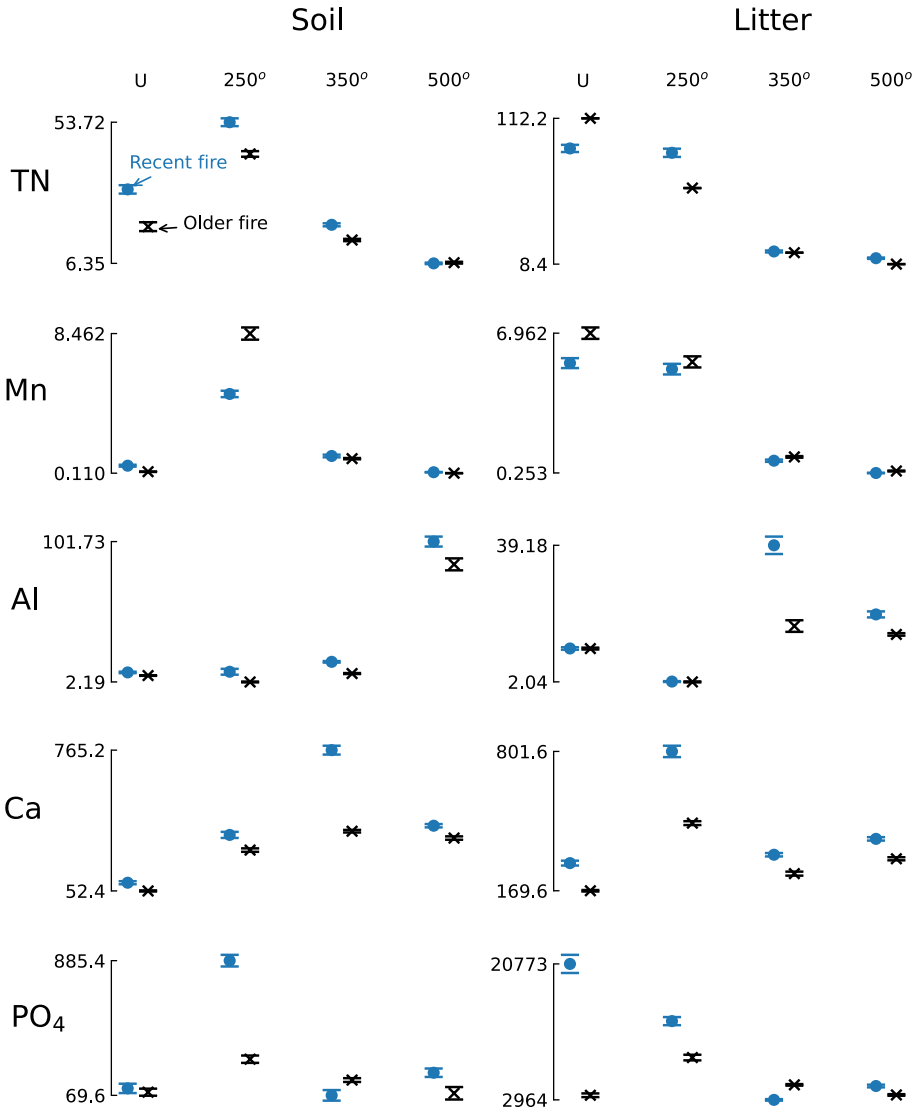


**Fig. 2.** Selected concentrations in soil and litter of untreated (U) and treated samples at different temperatures. The means (n = 15 for each subset) are bounded by a standard error of mean (horizontal line). The blue enclosed circle represents the recent, whereas the black X represents the older forest fire. The concentrations (y-axis) are in mg/kg of burnt matter.

centrations increase and (2) net solute loss, when the concentrations decline. Thus, if a concentration increases for the same element over the lower or medium temperature intervals (i.e. U-250°C and/or 250°C–350°C) followed by its decline at the high temperature interval (350°C–500°C), it indicates a net solute accumulation followed by a net solute loss. The net solute accumulation is a result of a prevalence of organic matter decomposition, mineral dissolution or desorption. The net solute decline is a consequence of dominating chemical precipitation, adsorption or emission. Moreover, if two constituents increase or decrease at the same temperature, this may indicate a common biogeochemical source or sink, respectively.

The soil seems to be more resistant to the loss of nutrients due to the temperature increase than litter. This is exemplified by TN and $PO_4^{3-}$, for which litter extracts show much steeper declines in concentrations when compared to soil. The same was found for TOC and TP (Appendix B).

With a few exceptions (e.g. Mn, Fig. 2), the recently burnt samples show higher concentrations that older burnt samples. This is particularly pronounced for primary macronutrients (TOC, TN, $PO_4^{3-}$ and K) and secondary macronutrients (Ca, Mg, S). Although total nutrient concentrations are higher in litter than in soils, the extracts from the recent burn for litter exhibit higher mean concentrations of TP, $PO_4^{3-}$ and K, but not TN, when compared to the older burn (Appendix B).

The two-way analysis of variance implies that all constituents are affected by *temperature* (Appendix C). *Time since last fire* is statistically significant for the primary macronutrients (TOC, TN, $PO_4^{3-}$ and K), secondary macronutrients (Ca, Mg, S), but not significant for micronutrients. The trend is stronger for soils than litter. On the contrary, time since last burn is statistically significant for pH in litter, but not for soils. The combination of *Temperature* and *Time since last fire* is important for the time-affected constituents and $NO_x$, but not significant for $SO_4^{2-}$ and K (Appendix C).

The Ca-$CO_3$ activity plot depicts chemical evolution of the organic matter conversion into inorganic carbon due to heating (Fig. 3). Its inspection also points to *differences and similarities* between the soils and the litter. For the soils, there is a significant enrichment (1 log unit) of $\gamma_{Ca^{2+}}$ in the temperature interval U-250°C, while $\gamma_{CO_3^{2-}}$ increases mostly in the temperature interval 250°C–350°C (1.5 log units). Also, there is a negligible difference between 350°C and 500°C for the soil $\gamma_{CO_3^{2-}}$. For the litter, there is a consistent enrichment in $\gamma_{CO_3^{2-}}$ throughout the whole temperature range (4 log units), while only a minor (0.5 log unit) increase of $\gamma_{Ca^{2+}}$ in the temperature interval U-250°C, which is reversed in 250°C–350°C. However, the general trends for the soils and litter are similar.

The higher (500°C, and some 350°C) temperature samples consistently plot above the $CaCO_3$ equilibrium lines, which corresponds to elevated pH values. The difference between the soils and litter manifests here too as the vast majority of the soil 350°C samples plot above the lines, implying the relative enrichment in $\gamma_{CO_3^{2-}}$, while most litter samples for this temperature lie below the $CaCO_3$ equilibrium lines.

The $CaCO_3$ equilibrium clearly controls the constituents that reveal concentration peaks at 250°C. For example, the highest concentrations of $Mn^{2+}$ occur upon the $\gamma_{Ca^{2+}}$ increase, but before the $\gamma_{CO_3^{2-}}$ increase. Thus, they consistently fall below the equilibrium line (Fig. 4). On the contrary, the behaviour of non-divalent ions like Al does not seem to be affected by elevated $\gamma_{CO_3^{2-}}$ (Fig. 4).

The samples at and above 350°C visually reacted with HCl and the presence of $CaCO_3$ was confirmed in the XRD profiles (Fig. 5). However, the relative differences of the diffraction angle $^o2\theta$ $CaCO_3$ at each temperatures are minor (46.08 in Fig. 5). Moreover, the profiles point to the existence of a phase or phases at $^o2\theta$ equal and larger than 80.55, which we attribute to SiC or organic chars, but the quantitative differences between the samples are minor.

## 4. Discussion

### 4.1. Calcium and carbonate activities as wildfire indicators

The results show that major ecological indicators of the degree of post-fire transformation are: $\gamma_{Ca^{2+}}$ and $\gamma_{CO_3^{2-}}$ that are derived from (1) pH, (2) alkalinity, and (3) $Ca^{2+}$ concentrations. The activities are calculated with Eqs. 1 and 2 by any thermodynamic software including PHREEQC.

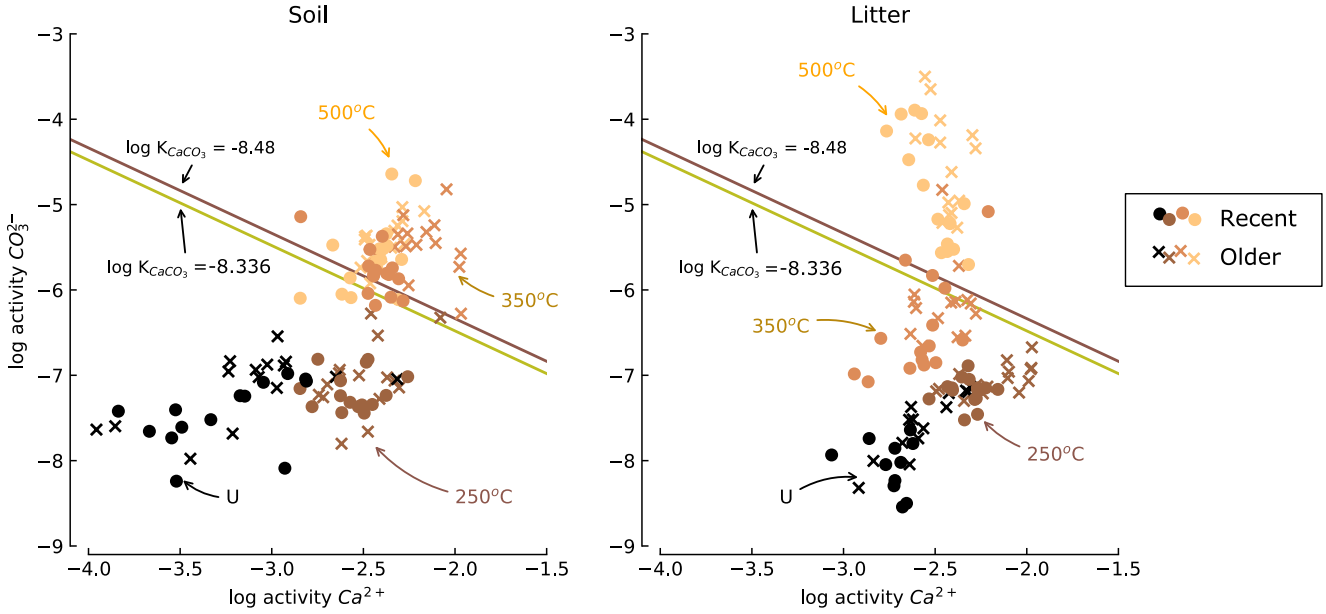


**Fig. 3.** The activities of calcium ($\gamma_{Ca^{2+}}$) and carbonates ($\gamma_{CO_3^{2-}}$) at different temperatures for soils (left) and litter (right) and the equilibrium for carbonate minerals (log K = −8.48 for calcite and log K = =-8.336 for aragonite). The medium and high temperature samples are affected by $CaCO_3$ precipitation. The highest concentrations plot below the $CaCO_3$ equilibrium lines.

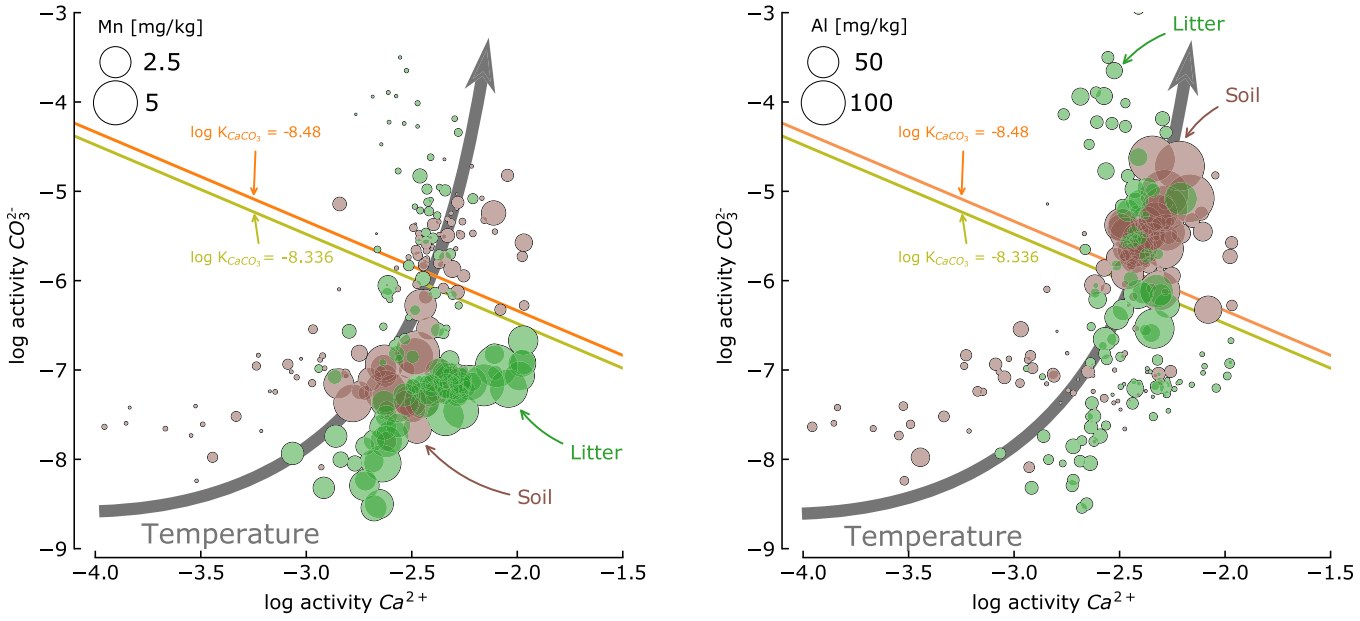


**Fig. 4.** Manganese and aluminium concentrations for soil and litter in the function of $\gamma_{Ca^{2+}}$ and $\gamma_{CO_3^{2-}}$. The lines indicate $CaCO_3$ equilibrium (log K = −8.48 for calcite and log K = =-8.336 for aragonite), with oversaturated conditions at the high $\gamma_{Ca^{2+}}$ and $\gamma_{CO_3^{2-}}$.

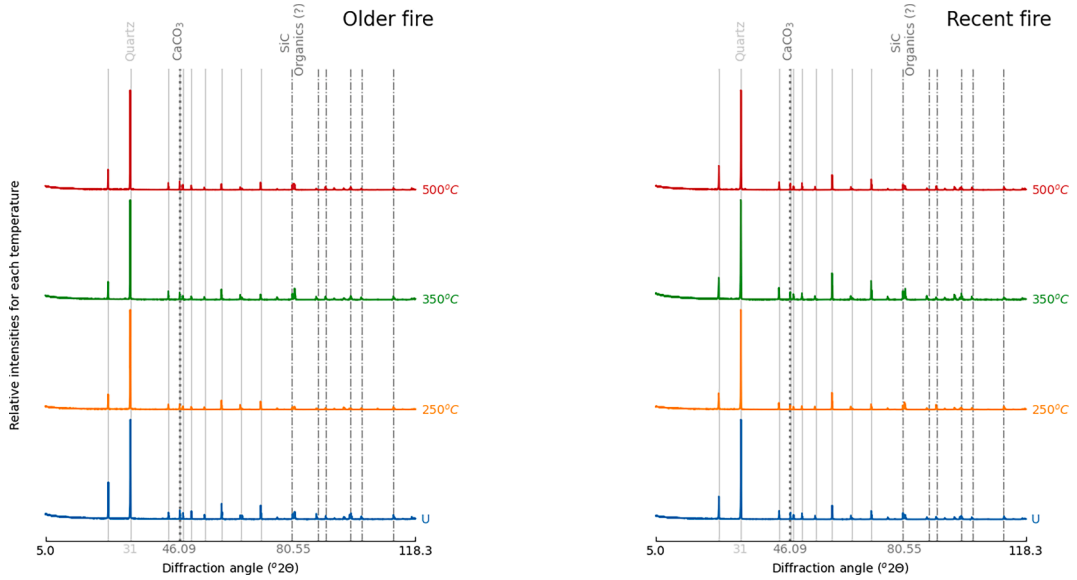


**Fig. 5.** XRD soil profiles indicating the dominance of quartz followed by SiC/organic material. $CaCO_3$ was confirmed in all samples. The older burn sample is 4B, while the more recent burn sample is 5E. Heating was applied for 30min.

Ionic strength can be calculated from electrical conductivity (EC) or a sum of dissolved solids. This means that the proposed indicators can be obtained without a need of analysing other post-wildfire concentrations.

The major advantages of the indicators include:

- they are good proxies for burn temperature and, consequently, for burn severity showing a significant spread in the temperature range U-500°C;
- they can be applied to both litter and soils debris even though the chemical composition of the unburnt sources are quite different;
- they are independent on the time since last fire;
- they may inform on other contaminants. Firstly $Ca^{2+}$ concentrations may be indicative of other divalent contaminants. Secondly, a high degree of burn, when $\gamma_{CO_3^{2-}}$ are high, implies a potential for Al and Cr contamination;
- pH, alkalinity and $Ca^{2+}$ concentrations are easy to measure in majority of wildfire scenarios;
- they can be calculated both for ash extracts and for water samples.

### 4.2. Low temperature resulting in high concentrations

Our experiment confirms that low temperature burns are likely to contribute to higher concentrations for many elements (Alcaniz et al., 2018; Neary, 2019; Úbeda et al., 2009; Pereira et al., 2014; Santín et al., 2015; Fajković et al., 2022). Since different vegetation types generate different chemical compositions of ash, the differences between the results seem to be site specific. Different vegetation is likely to influence

chemical stocks of the soils (Alcaniz et al., 2018; Neary, 2019).

Our results clearly demonstrate that incomplete combustion of organic matter at 250°C and 350°C along with mineral transformations is responsible for solute liberation at low temperature burns. This has an important implication that the temperature itself influences solute leaching. The combination of environmental factors such as (1) burn temperature, (2) topography, (3) rainfall and its chemistry, (4) vegetation and soils, (5) the area affected by a burn, (6) the volume of ash generated, and (7) the hydrological conditions must then explain why increased concentrations for low-severity burns are rarely identified in field conditions. In a field study, Santín et al. (2018) who compared unburnt sites with low-, medium- and high severity burns found that only Ca and Cu were elevated for low severity burn.

### 4.3. Chemical precipitation as an important biogeochemical sink

We show that $CaCO_3$ precipitation affects both soil and litter samples. The process is quite common in post-wildfire environs (Úbeda et al., 2009; Pereira et al., 2012; Bodí et al., 2014) and it was confirmed in the SW Australia lateritic soil following a high-severity fire (Yusiharni and Gilkes, 2012). The increase in alkalinity at 250°C–350°C roughly correspond to a 2–3.5 fold increase in carbonate content in *darkened soil* compared to the unburnt soil in southern California forest (Goforth et al., 2005). Santín et al. (2015) did not report on $CaCO_3$ presence in post-wildfire ashes from SE Australia, but the increase in soluble $Ca^{2+}$ for the low-severity burn, followed by its decline at the high-severity burn points to the accumulation of the phase.

The $CaCO_3$ formation has broader implications through co-precipitation and sorption. It coincides at 250350°C–°C with the absence of Mn (Fig. 4) and divalent metals (Zn, Ni, not shown) that are normally associated with Mn-oxides. Since the unburnt samples are stable for the two most common manganese oxides (pyrolusite and birnessite Fig. D.8), Mn-oxides are a possible source of the metals. Also, Mn-rich organic matter may be releasing these metals at the lowest temperature (U-250°C). At these temperatures, thermal decomposition was observed in laboratory studies for both Mn-oxides (Min and Kim, 2020; Gaillot et al., 2005) and organic matter (Johnson et al., 2015). Another explanation for Mn mobilisation is cation exchange associated with $CaCO_3$ precipitation. Since cation exchange capacity is expected to be much higher for soils than for litter, if cation exchange was a dominant mechanism, different patterns for soil and litter would be observed. At the medium and higher temperatures, $Mn^{2+}$ and other divalent cations may then get incorporated into the $CaCO_3$ crystal lattice (Son and Newton, 2019). The formation of $CaCO_3$ may also be responsible for the $PO_4^{3-}$ decline at 250°C–350°C. Although, $PO_4^{3-}$ gets strongly adsorbed to freshly precipitated $CaCO_3$ without incorporation to the crystal lattice (Sø et al., 2011), both phosphorus-rich calcite and apatite were found in post-wildfire soils at a nearby location (Yusiharni and Gilkes, 2012).

Whilst Fe often resembles the behaviour of $Mn^{2+}$, $Ca^{2+}$, $Mg^{2+}$ and $PO_4^{3-}$ in aquatic environs (Stumm and Morgan, 2013), we observed that soluble Fe is absent in the temperature interval U-250°C and continues to be absent in higher temperatures. This is different than observed in SE Australia, where Fe was found at higher temperatures (Santín et al., 2015). If the Fe absence was associated with $CaCO_3$ precipitation in our experiment, some Fe would be expected in the soluble form at 250°C. However, a possible mechanism for Fe immobilisation is a thermal transformation of iron oxides. Nørnberg et al. (2009), by performing Mössbauer spectroscopy of soil which underwent long-term heating, showed the transformation of ferrihydrite and goethite to hematite from around 100°C peak temperature and the transformation from hematite to maghemite at around 300°C peak temperature. Johnston et al. (2019) shows that at the exposure to 400°C both ferrihydrite and goethite were significantly transformed to hematite and maghemite, respectively, within 60min of heating. Thus, we claim that Fe, probably along with Pb and Cd as they become absent too, is lost at U-250°C due to formation of more stable phases. Johnston et al. (2018, 2019) showed Fe and As incorporation into the stable Fe-oxides during heating. Contrary to Nørnberg et al. (2009) and Yusiharni and Gilkes (2012), we could not observe any maghemite/hematite increase through XRD even at the highest temperature (Fig. 5). This may be related with a much shorter heating duration (30min) when compared with (Nørnberg et al., 2009; Yusiharni and Gilkes, 2012). Also, Johnston et al. (2019) indicated very small XRD quantitative differences for heating duration shorter than 60min. An alternative for the Fe absence is its adsorption at the low temperature on char (Liu et al., 2017), however it is difficult to explain as to why it would be affected more than other cations. Nevertheless, further research on the role of char on solute behaviour in wildfire conditions is warranted (Smith et al., 2011; Bodí et al., 2014).

### 4.4. Soils are a significant source of dissolved contamination

The number of potential contaminants present in higher levels in soils than in litter (Fe, Mn, Zn, Al, Cr, $SO_4^{2-}$), indicates that post-fire soil could be considered as a contamination source (Fig. B.6 and B.7 in Appendix B). Our study shows Al and Cr are generated at the high (500°C) temperature, as well as Mn, Zn and As which are developed at low (250°C) and medium (350°C) temperatures.

The elevated soil Al concentrations ($94 \pm 58$ mg $kg^{-1}$) at the highest temperature are lower than reported by Santín et al. (2015), but the increasing trend found in both cases indicates that high severity fires result in the release of Al. The Al concentrations and the pH at 500°C slightly exceed the equilibrium with gibbsite ($Al(OH)_3$, not shown) implying that higher dissolved Al concentrations are not expected at these pH values. However, if at higher pH values, Al is likely to be higher.

The behaviour of Al is followed by leachable Cr ($50 \pm 47$ μg $kg^{-1}$). Much higher total Cr concentrations ($> 350$ mg $kg^{-1}$) in post-wildfire ash were reported after the Harris fire in California in 2007 (Wolf et al., 2008). Although there is an association of $Cr^{6+}$ mobilisation with the stability of Mn-oxides (Oze et al., 2007), we did not observe elevated Cr at lower temperatures when the Mn liberation takes place. This implies that organic matter rather than Mn-oxides is the source of Cr. The Cr sink is also different than Mn, as Cr does not decline at low (250°C) and middle (350°C) temperatures. This may suggest the Cr association with iron oxides as observed by Thery et al. (2023).

Although the soil concentrations of Mn, Zn and As were much higher than in litter, the highest concentrations occurred at higher temperatures in soils than in litter, which confirms that soils are generally more resistant to higher temperatures than litter (Alcaniz et al., 2018). The thermal resistance also applies to TN and DOC, although their concentrations in soil are generally lower than in litter.

The soil contamination along with hydrological and meteorological triggers may consequently affect drinking water quality. There is a particular concern that soils of the jarrah forest, in which eucalyptus species dominate, become more hydrophobic after fire increasing the potential for soil erosion and consequent degradation of water quality (Mao et al., 2019; Blake et al., 2020). Thus, there is a need to determine in field studies how increased temperature and duration of fire affect infiltration in jarrah forest through spatio-temporal changes in (1) soil hydrophobicity, (2) soil moisture, and (3) a potential formation of preferential pathways.

### 4.5. Recent fires affect water quality

Higher concentrations for the recent burn, when compared to the older burn indicate that the *Time since last fire* is significant for solute leaching. The higher concentrations explain fast leaf area index (LAI) increases following jarrah forest fires (Boer et al., 2008).

Relatively high concentrations for the recent burn just a couple of months following a wet winter season indicate that the shallow soils of

the jarrah forest had capability in maintaining nutrients in soil. A similar recuperation was not found in the frequently burnt wet sclerophyll forest in SE Queensland, Australia (Muqaddas et al., 2015). Thus, it is important to evaluate (1) how the recurrence of frequent burns affects this capability, and (2) whether the same is observed when sampling fresh wildfire matter in the jarrah forest.

Higher pH of burnt litter in the more recent burns is in agreement with a few field studies (Neill et al., 2007; Yusiharni and Gilkes, 2012; Alcaniz et al., 2018). It is important to determine how the pH shift affects both biogeochemical and microbiological functioning of the forested systems (Stegen, 2018; Johnson et al., 2015; Pellegrini et al., 2022).

The time since last fire does not affect the wildfire indicators (Fig. 3). Although $CaCO_3$ was identified by XRD for both unburnt and treated soils (Fig. 5), it is expected that water flushing easily removes $CaCO_3$, while burning readily replenishes soil with $CaCO_3$. $CaCO_3$ precipitation is not apparent in low-pH wetland soils (Blake et al., 2021).

## 5. Conclusions

Burn temperature is one of the crucial factors controlling post-wildfire water quality, although its measurement at suitable spatial and temporal scales remains a significant challenge. Moreover, its influence on soil and litter is site specific and depends on vegetation, soil chemistry, climate and hydrology among other factors. A set of ecological indicators ($\gamma_{Ca^{2+}}$ and $\gamma_{CO_3^{2-}}$) outlined in this contribution offers a pathway to simplify the complexity of post-fire environs.

Although we suggest that our set of ecological indicators provides novel insights, it is important to recognise that there are limitations and, as with any new approach, these limitations can be vetted through additional use and different scale studies. Firstly, the approach needs to verified in the field. Secondly, it needs to be tested against organic contaminants that offer a significant water quality thread. Finally, it needs to be validated in other geographical settings.

## CRediT authorship contribution statement

**Konrad Miotliński:** Conceptualization, Methodology, Formal analysis, Investigation, Data curation, Writing - original draft, Visualization. **Kuenzang Tshering:** Conceptualization, Data curation, Writing - review & editing. **Mary C. Boyce:** Conceptualization, Methodology, Writing - review & editing. **David Blake:** Conceptualization, Writing - review & editing, Funding acquisition, Project administration. **Pierre Horwitz:** Conceptualization, Investigation, Supervision, Writing - review & editing, Funding acquisition, Project administration.

## Declaration of Competing Interest

The authors declare the following financial interests/personal relationships which may be considered as potential competing interests: Konrad Miotlinski reports financial support was provided by Water Corporation.

## Data availability

Data will be made available on request.

## Acknowledgements

The authors are grateful to the Water Corporation of Western Australia for funding the project (Predicting Impact of Fires on Water Quality), and to Mrs. Jacquie Bellhouse, Dr. Andrew Bath and Ms. Amanda Mitchell for their project management contributions. Ms. Robyn Babin and Mr. Matthew Giraudo (Water Corporation of Western Australia) are acknowledged for facilitating access to the sampling sites. Kuenzang Tshering's involvement is funded through Edith Cowan University Higher Degree by Research Scholarship.

## Appendix A. Supplementary data

Supplementary data associated with this article can be found, in the online version, athttps://doi.org/10.1016/j.ecolind.2023.110236.

## References

Abram, N.J., Abram, N.J., Henley, B.J., Gupta, A.S., Lippmann, T.J., Clarke, H., Dowdy, A.J., Sharples, J.J., Nolan, R.H., Zhang, T., Wooster, M.J., Wurtzel, J.B., Meissner, K.J., Pitman, A.J., Ukkola, A.M., Murphy, B.P., Tapper, N.J., Boer, M.M., 2021. Connections of climate change and variability to large and extreme forest fires in southeast Australia. Commun. Earth Environ. 2 https://doi.org/10.1038/s43247-020-00065-8.

Alcaniz, M., Outeiro, L., Francos, M., Úbeda, X., 2018. Effects of prescribed fires on soil properties: A review. Sci. Total Environ. 613–614, 944–957. https://doi.org/10.1016/j.scitotenv.2017.09.144.

Anand, R.R., Gilkes, R.J., 1987. Iron oxides in lateritic soils from Western Australia. J. Soil Sci. 38, 607–622.

Anand, R.R., Hough, R.M., Salama, W., Aspandiar, M.F., Butt, C.R.M., González-Álvarez, I., Metelka, V., 2019. Gold and pathfinder elements in ferricrete gold deposits of the Yilgarn Craton of Western Australia: A review with new concepts. Ore Geol. Rev. 104, 294–355. https://doi.org/10.1016/j.oregeorev.2018.11.003. URL: http://www.sciencedirect.com/science/article/pii/S0169136818305729.

Appelo, C.A.J., & Postma, D. (2005). Geochemistry, Groundwater and Pollution, Second Edition. Taylor & Francis. URL: https://www.taylorfrancis.com/books/9781439833544. DOI: 10.1201/9781439833544.

Archibald, S., Lehmann, C.E.R., Belcher, C.M., Bond, W.J., Bradstock, R.A., Daniau, A.-L., Dexter, K.G., Forrestel, E.J., Greve, M., He, T., Higgins, S.I., Hoffmann, W.A., Lamont, B.B., McGlinn, D.J., Moncrieff, G.R., Osborne, C.P., Pausas, J.G., Price, O., Ripley, B.S., Rogers, B.M., Schwilk, D.W., Simon, M.F., Turetsky, M.R., der Werf, G. R.V., & Zanne, A.E. (2018). Biological and geophysical feedbacks with fire in the earth system. Environmental Research Letters, 13, 033003. URL: doi: 10.1088/1748-9326/aa9ead. DOI: 10.1088/1748-9326/aa9ead.

Blake, D., Boyce, M.C., Stock, W.D., Horwitz, P., 2021. Fire in organic-rich wetland sediments: Inorganic responses in porewater. Water, Air, Soil Pollut. 232 https://doi.org/10.1007/s11270-021-05013-6.

Blake, D., Nyman, P., Nice, H., D'souza, F.M., Kavazos, C.R., Horwitz, P., 2020. Assessment of post-wildfire erosion risk and effects on water quality in south-western australia. Int. J. Wildland Fire 29, 240–257. https://doi.org/10.1071/WF18123.

Bodí, M.B., Martin, D.A., Balfour, V.N., Santín, C., Doerr, S.H., Pereira, P., Cerdá, A., & Mataix-Solera, J. (2014). Wildland fire ash: Production, composition and eco-hydro-geomorphic effects. Earth-Science Reviews, 130, 103–127. URL: doi: 10.1016/j.earscirev.2013.12.007. DOI: 10.1016/j.earscirev.2013.12.007.

Boer, M.M., Macfarlane, C., Norris, J., Sadler, R.J., Wallace, J., Grierson, P.F., 2008. Mapping burned areas and burn severity patterns in SW Australian eucalypt forest using remotely-sensed changes in leaf area index. Remote Sens. Environ. 112, 4358–4369. https://doi.org/10.1016/j.rse.2008.08.005. URL: https://www.sciencedirect.com/science/article/pii/S0034425708002484.

Bradstock, R.A., Auld, T.D., 1995. Soil temperatures during experimental bushfires in relation to fire intensity: Consequences for legume germination and fire management in south-eastern Australia. J. Appl. Ecol. 32, 76–84.

Burton, E.D., Choppala, G., Vithana, C.L., Karimian, N., Hockmann, K., & Johnston, S.G. (2019). Chromium(VI) formation via heating of Cr(III)-Fe(III)-(oxy)hydroxides: A pathway for fire-induced soil pollution. Chemosphere, 222, 440–444. URL: doi: 10.1016/j.chemosphere.2019.01.172. DOI: 10.1016/j.chemosphere.2019.01.172.

Campos, I., Abrantes, N., Keizer, J.J., Vale, C., Pereira, P., 2016. Major and trace elements in soils and ashes of eucalypt and pine forest plantations in Portugal following a wildfire. Sci. Total Environ. 572, 1363–1376. https://doi.org/10.1016/j.scitotenv.2016.01.190.

Chen, H., Wang, J.J., Ku, P.J., Tsui, M.T.K., Abney, R.B., Berhe, A.A., Zhang, Q., Burton, S.D., Dahlgren, R.A., Chow, A.T., 2022. Burn intensity drives the alteration of phenolic lignin to (poly) aromatic hydrocarbons as revealed by pyrolysis gas chromatography-mass spectrometry (py-gc/ms). Environ. Sci. Technol. 56, 12678–12687. https://doi.org/10.1021/acs.est.2c00426.

Churchward, H., & Dimmock, G. (1989). The soils and landforms of the northern jarrah forest. In The Jarrah Forest (pp. 13–21).

Clavijo, S.P., Addassi, M., Finkbeiner, T., Hoteit, H., 2022. A coupled phase-field and reactive-transport framework for fracture propagation in poroelastic media. Sci. Rep. 12 https://doi.org/10.1038/s41598-022-22684-1.

Coughlan, K., Cresswell, H., & McKenzie, N. (2002). Soil Physical Measurement and Interpretation for Land Evaluation. CSIRO Publishing. URL: https://ebooks.publish.csiro.au/content/9780643069879/9780643069879. 10.1071/9780643069879.

Davis, J.C., 2002. Statistics and data analysis in geology. Wiley and Sons.

Dell, J.J., & Havel, B. (1989). The jarrah forest, an introduction. In havel1989jarrah. URL: doi: 10.1007/978-94-009-3111-4_1. DOI: 10.1007/978-94-009-3111-4_1.

Demirel, Y., Gerbaud, V., 2019. Chapter 1 - fundamentals of equilibrium thermodynamics. In: Demirel, Y., Gerbaud, V. (Eds.), Nonequilibrium Thermodynamics, Fourth edition ed. Elsevier, pp. 1–85. https://doi.org/10.1016/B978-0-444-64112-0.00001-0.

Doebelin, N., Kleeberg, R., 2015. Profex: A graphical user interface for the rietveld refinement program bgmn. J. Appl. Crystallogr. 48, 1573–1580. https://doi.org/10.1107/S1600576715014685.
Eldridge, D.J., Maestre, F.T., Koen, T.B., Delgado-Baquerizo, M., 2018. Australian dryland soils are acidic and nutrient-depleted, and have unique microbial communities compared with other drylands. J. Biogeogr. 45, 2803–2814. https://doi.org/10.1111/jbi.13456.
Fajković, H., Ivanić, M., Nemet, I., Roncević, S., Kampić, S., Vazdar, D.L., 2022. Heat-induced changes in soil properties: Fires as cause for remobilization of chemical elements. J. Hydrol. Hydromech. 70, 421–431. https://doi.org/10.2478/johh-2022-0024.
Gaillot, A.C., Lanson, B., Drits, V.A., 2005. Structure of birnessite obtained from decomposition of permanganate under soft hydrothermal conditions. 1. chemical and structural evolution as a function of temperature. Chem. Mater. 17, 2959–2975. https://doi.org/10.1021/cm0500152.
Goforth, B.R., Graham, R.C., Hubbert, K.R., Zanner, C.W., Minnich, R.A., 2005. Spatial distribution and properties of ash and thermally altered soils after high-severity forest fire, southern California. Int. J. Wildland Fire 14, 343–354. https://doi.org/10.1071/WF05038.
Havel, J., Dell, B., Malajczuk, N., 1989. The jarrah forest: a complex Mediterranean ecosystem. Kluwer Academic Publishers.
Havel, J.J. (1989). Conservation in the northern jarrah forest. In havel1989jarrah. URL: doi: 10.1007/978-94-009-3111-4_20. DOI: 10.1007/978-94-009-3111-4_20.
Johnson, K., Purvis, G., Lopez-Capel, E., Peacock, C., Gray, N., Wagner, T., März, C., Bowen, L., Ojeda, J., Finlay, N., Robertson, S., Worrall, F., Greenwell, C., 2015. Towards a mechanistic understanding of carbon stabilization in manganese oxides. Nature Commun. 6 https://doi.org/10.1038/ncomms8628.
Johnston, S.G., Bennett, W.W., Burton, E.D., Hockmann, K., Dawson, N., Karimian, N., 2018. Rapid arsenic(v)-reduction by fire in schwertmannite-rich soil enhances arsenic mobilisation. Geochim. Cosmochim. Acta 227, 1–18. https://doi.org/10.1016/j.gca.2018.01.031.
Johnston, S.G., Karimian, N., Burton, E.D., 2019. Fire promotes arsenic mobilization and rapid arsenic(III) formation in soil via thermal alteration of arsenic-bearing iron oxides. Frontiers in Earth Science 7, 1–18. https://doi.org/10.3389/feart.2019.00139.
Lee, M., Gomez, M.G., Pablo, A.C.S., Kolbus, C.M., Graddy, C.M., DeJong, J.T., Nelson, D. C., 2019. Investigating ammonium by-product removal for ureolytic bio-cementation using meter-scale experiments. Sci. Rep. 9 https://doi.org/10.1038/s41598-019-54666-1.
Li, L., Sullivan, P.L., Benettin, P., Cirpka, O.A., Bishop, K., Brantley, S.L., Knapp, J.L.A., Meerveld, I., Rinaldo, A., Seibert, J., Wen, H., & Kirchner, J.W. (2020). Toward catchment hydro–biogeochemical theories. WIREs Water, URL: https://onlinelibrary.wiley.com/doi/10.1002/wat2.1495. DOI: 10.1002/wat2.1495.
Li, R., Liu, C., Jiao, P., Hu, Y., Liu, W., Wang, S., 2021. Simulation study on the mining conditions of dissolution of low grade solid potash ore in Qarhan Salt Lake. Scientific Reports 11. https://doi.org/10.1038/s41598-021-88818-z.
Liu, W.J., Li, W.W., Jiang, H., Yu, H.Q., 2017. Fates of chemical elements in biomass during its pyrolysis. Chem. Rev. 117, 6367–6398. https://doi.org/10.1021/acs.chemrev.6b00647.
Manning, D., 2005. Waste disposal on land — municipal. In: Hillel, D. (Ed.), Encyclopedia of Soils in the Environment. Elsevier, Oxford, pp. 247–252. https://doi.org/10.1016/B0-12-348530-4/00103-X. URL: https://www.sciencedirect.com/science/article/pii/B012348530400103X.
Mao, J., Nierop, K.G.J., Dekker, S.C., 2019. W., D.L., & Chen, B. Understanding the mechanisms of soil water repellency from nanoscale to ecosystem scale: a review. J. Soils Sediments 19, 171–185. https://doi.org/10.1007/s11368-018-2195-9.
McLauchlan, K.K., Higuera, P.E., Miesel, J., Rogers, B.M., Schweitzer, J., Shuman, J.K., Tepley, A.J., Varner, J.M., Veblen, T.T., Adalsteinsson, S.A., Balch, J.K., Baker, P., Batllori, E., Bigio, E., Brando, P., Cattau, M., Chipman, M.L., Coen, J., Crandall, R., Daniels, L., Enright, N., Gross, W.S., Harvey, B.J., Hatten, J.A., Hermann, S., Hewitt, R.E., Kobziar, L.N., Landesmann, J.B., Loranty, M.M., Maezumi, S.Y., Mearns, L., Moritz, M., Myers, J.A., Pausas, J.G., Pellegrini, A.F., Platt, W.J., Roozeboom, J., Safford, H., Santos, F., Scheller, R.M., Sherriff, R.L., Smith, K.G., Smith, M.D., Watts, A.C., 2020. Fire as a fundamental ecological process: Research advances and frontiers. J. Ecol. 108, 2047–2069. https://doi.org/10.1111/1365-2745.13403.
Min, S., Kim, Y., 2020. Physicochemical characteristics of the birnessite and todorokite synthesized using various methods. Minerals 10, 1–17. https://doi.org/10.3390/min10100884.
Mishra, A., Alnahit, A., Campbell, B., 2021. Impact of land uses, drought, flood, wildfire, and cascading events on water quality and microbial communities: A review and analysis. J. Hydrol. 596 https://doi.org/10.1016/j.jhydrol.2020.125707.
Mongin, M., Baird, M.E., Tilbrook, B., Matear, R.J., Lenton, A., Herzfeld, M., Wild-Allen, K., Skerratt, J., Margvelashvili, N., Robson, B.J., Duarte, C.M., Gustafsson, M. S., Ralph, P.J., Steven, A.D., 2016. The exposure of the Great Barrier Reef to ocean acidification. Nature Communications 7. https://doi.org/10.1038/ncomms10732.
Moody, J.A., Ebel, B.A., 2012. Hyper-dry conditions provide new insights into the cause of extreme floods after wildfire. Catena 93, 58–63. https://doi.org/10.1016/j.catena.2012.01.006.
Mooshammer, M., Hofhansl, F., Frank, A.H., Wanek, W., Hämmerle, I., Leitner, S., Schnecker, J., Wild, B., Watzka, M., Keiblinger, K.M., Zechmeister-Boltenstern, S., & Richter, A. (2017). Decoupling of microbial carbon, nitrogen, and phosphorus cycling in response to extreme temperature events. Science Advances, 3, e1602781. URL: https://www.science.org/doi/abs/10.1126/sciadv.1602781. DOI: 10.1126/sciadv.1602781. arXiv:https://www.science.org/doi/pdf/10.1126/sciadv.1602781.
Muqaddas, B., Zhou, X., Lewis, T., Wild, C., Chen, C., 2015. Long-term frequent prescribed fire decreases surface soil carbon and nitrogen pools in a wet sclerophyll forest of southeast queensland, australia. Sci. Total Environ. 536, 39–47. https://doi.org/10.1016/j.scitotenv.2015.07.023.
Nagra, G., Treble, P.C., Andersen, M.S., Bajo, P., Hellstrom, J., Baker, A., 2017. Dating stalagmites in mediterranean climates using annual trace element cycles. Sci. Rep. 7, 1–12. https://doi.org/10.1038/s41598-017-00474-4.
Neary, D.G., 2019. Forest soil disturbance: Implications of factors contributing to the wildland fire nexus. Soil Sci. Soc. Am. J. 83 https://doi.org/10.2136/sssaj2018.12.0471.
Neill, C., Patterson, W.A., Crary, D.W., 2007. Responses of soil carbon, nitrogen and cations to the frequency and seasonality of prescribed burning in a Cape Cod oak-pine forest. For. Ecol. Manage. 250, 234–243. https://doi.org/10.1016/j.foreco.2007.05.023.
Newland, M.J., Ren, Y., Mcgillen, M.R., Michelat, L., Daële, V., Mellouki, A., 2022. NO3 chemistry of wildfire emissions: A kinetic study of the gas-phase reactions of furans with the NO3 radical. Atmos. Chem. Phys. 22, 1761–1772. https://doi.org/10.5194/acp-22-1761-2022.
Nunes, J.P., Doerr, S.H., Sheridan, G., Neris, J., Santín, C., Emelko, M.B., Silins, U., Robichaud, P.R., Elliot, W.J., Keizer, J., 2018. Assessing water contamination risk from vegetation fires: Challenges, opportunities and a framework for progress. Hydrol. Process. 32, 687–694. https://doi.org/10.1002/hyp.11434.
Nørnberg, P., Vendelboe, A.L., Gunnlaugsson, H.P., Merrison, J.P., Finster, K., Jensen, S. K., 2009. Comparison of the mineralogical effects of an experimental forest fire on a goethite/ferrihydrite soil with a topsoil that contains hematite, maghemite and goethite. Clay Miner. 44, 239–247. https://doi.org/10.1180/claymin.2009.044.2.239.
Oze, C., Bird, D.K., & Fendorf, S. (2007). Genesis of hexavalent chromium from natural sources in soil and groundwater. PNAS,. URL: https://doi.org/10.1073/pnas.0701085104.
Parkhurst, D.L., & Appelo, C.A.J. (2013). Description of input and examples for PHREEQC version 3–A computer program for speciation, batch-reaction, one-dimensional transport, and inverse geochemical calculations. Technical Report U.S. Geological Survey Techniques and Method, book 6 chap A43. URL: https://www.usgs.gov/software/phreeqc-version-3. doi: 10.3133/tm6A43.
Pellegrini, A.F., Ahlström, A., Hobbie, S.E., Reich, P.B., Nieradzik, L.P., Staver, A.C., Scharenbroch, B.C., Jumpponen, A., Anderegg, W.R., Randerson, J.T., Jackson, R.B., 2018. Fire frequency drives decadal changes in soil carbon and nitrogen and ecosystem productivity. Nature 553. https://doi.org/10.1038/nature24668.
Pellegrini, A.F., Harden, J., Georgiou, K., Hemes, K.S., Malhotra, A., Nolan, C.J., Jackson, R.B., 2022. Fire effects on the persistence of soil organic matter and long-term carbon storage. Nat. Geosci. 15, 5–13. https://doi.org/10.1038/s41561-021-00867-1.
Pereira, P., Úbeda, X., Martin, D.A., 2012. Fire severity effects on ash chemical composition and water-extractable elements. Geoderma 191, 105–114. https://doi.org/10.1016/j.geoderma.2012.02.005.
Pereira, P., Úbeda, X., Martin, D., Mataix-Solera, J., Cerdá, A., Burguet, M., 2014. Wildfire effects on extractable elements in ash from a pinus pinaster forest in Portugal. Hydrol. Process. 28, 3681–3690. https://doi.org/10.1002/hyp.9907.
Postma, D., 1983. Pyrite and siderite oxidation in swamp sediments. J. Soil Sci. 34, 163–182. https://doi.org/10.1111/j.1365-2389.1983.tb00821.x.
Raoelison, O.D., Valenca, R., Lee, A., Karim, S., Webster, J.P., Poulin, B.A., Mohanty, S. K., 2023. Wildfire impacts on surface water quality parameters: Cause of data variability and reporting needs. Environ. Pollut. 317 https://doi.org/10.1016/j.envpol.2022.120713.
Robinne, F.N., Hallema, D.W., Bladon, K.D., Flannigan, M.D., Boisramé, G., Bréthaut, C. M., Doerr, S.H., Baldassarre, G.D., Gallagher, L.A., Hohner, A.K., Khan, S.J., Kinoshita, A.M., Mordecai, R., Nunes, J.P., Nyman, P., Santín, C., Sheridan, G., Stoof, C.R., Thompson, M.P., Waddington, J.M., Wei, Y., 2021. Scientists' warning on extreme wildfire risks to water supply. Hydrol. Process. 35 https://doi.org/10.1002/hyp.14086.
Roshan, A., Biswas, A., 2023. Fire-induced geochemical changes in soil: Implication for the element cycling. Science of The Total Environment 868, 161714. https://doi.org/10.1016/j.scitotenv.2023.161714.
Santín, C., Doerr, S.H., Otero, X.L., Chafer, C.J., 2015. Quantity, composition and water contamination potential of ash produced under different wildfire severities. Environ. Res. 142, 297–308. https://doi.org/10.1016/j.envres.2015.06.041.
Santín, C., Otero, X.L., Doerr, S.H., Chafer, C.J., 2018. Impact of a moderate/high-severity prescribed eucalypt forest fire on soil phosphorous stocks and partitioning. Sci. Total Environ. 621, 1103–1114. https://doi.org/10.1016/j.scitotenv.2017.10.116.
Santos, F., Wymore, A.S., Jackson, B.K., Sullivan, S.M.P., McDowell, W.H., Berhe, A.A., 2019. Fire severity, time since fire, and site-level characteristics influence streamwater chemistry at baseflow conditions in catchments of the sierra nevada, california, usa. Fire Ecology 15. https://doi.org/10.1186/s42408-018-0022-8.
Santucci, R.J., & Scully, J.R. (2020). The pervasive threat of lead (Pb) in drinking water: Unmasking and pursuing scientific factors that govern lead release. Proceedings of the National Academy of Sciences of the United States of America, 117, 23211–23218. DOI: 10.1073/pnas.1913749117.
Smith, H.G., Sheridan, G.J., Lane, P.N., Nyman, P., Haydon, S., 2011. Wildfire effects on water quality in forest catchments: A review with implications for water supply. J. Hydrol. 396, 170–192. https://doi.org/10.1016/j.jhydrol.2010.10.043.
Sø, H.U., Postma, D., Jakobsen, R., Larsen, F., 2011. Sorption of phosphate onto calcite; results from batch experiments and surface complexation modeling. Geochim. Cosmochim. Acta 75, 2911–2923. https://doi.org/10.1016/j.gca.2011.02.031. URL: https://www.sciencedirect.com/science/article/pii/S0016703711001116.

Son, S., Newton, A.G., Kyoung-nam, J., Lee, J.Y., Kwon, K.D., 2019. Manganese speciation in mn-rich caco 3: A density functional theory study. Geochim. Cosmochim. Acta 248, 231–241. https://doi.org/10.1016/j.gca.2019.01.011.

Stegen, J.C., 2018. At the nexus of history, ecology, and hydrobiogeochemistry: Improved predictions across scales through integration. mSystems 3, 1–8. https://doi.org/10.1128/msystems.00167-17.

Stumm, W., & Morgan, J.J. (2013). Aquatic chemistry: chemical equilibria and rates in natural waters volume 33. 10.5860/choice.33-6312.

Thery, G., Juillot, F., Meyer, M., Quiniou, T., David, M., Jourand, P., Ducousso, M., Fritsch, E., 2023. Wildfires on cr-rich ferralsols can cause freshwater cr(vi) pollution: A pilot study in new caledonia. Appl. Geochem. 148 https://doi.org/10.1016/j.apgeochem.2022.105513.

Tshering, K., Miotlinski, K., Blake, D., Boyce, M.C., Bath, A., Carvalho, A., Horwitz, P., 2023. Effect of fire on characteristics of dissolved organic matter in forested catchments in the mediterranean biome: A review. Water Res. 230, 119490 https://doi.org/10.1016/j.watres.2022.119490. URL: https://www.sciencedirect.com/science/article/pii/S004313542201435X.

Úbeda, X., Pereira, P., Outeiro, L., Martin, D.A., 2009. Effects of fire temperature on the physical and chemical characteristics of the ash from two plots of cork oak (quercus suber). Land Degrad. Dev. 20, 589–608. https://doi.org/10.1002/ldr.930.

Wolf, R.E., Morman, S.A., Plumlee, G.S., Hageman, P.L., & Adams, M. (2008). Release of Hexavalent Chromium by Ash and Soils in Wildfire-Impacted Areas. Technical Report USGS Open-File Report. URL: http://pubs.usgs.gov/tm/2007/05D03/.

Yusiharni, E., Gilkes, R., 2012. Minerals in the ash of australian native plants. Geoderma 189–190, 369–380. https://doi.org/10.1016/j.geoderma.2012.06.035.

Yusiharni, E., Gilkes, R.J., 2012. Changes in the mineralogy and chemistry of a lateritic soil due to a bushfire at wundowie, darling range, western australia. Geoderma 191, 140–150. https://doi.org/10.1016/j.geoderma.2012.01.030.